Supplemental Data. Rodriguez et al. Plant Cell (2014) 10.1105/tpc.114.129973

Supplemental Figure 1. Scheme of some representative proteins harboring C2 domains in *Arabidopsis*. A total of 123 proteins containing one or several C2 domains were identified in TAIR using the SMART tool (http://smart.embl-heidelberg.de/) (Schultz et al., 1988). The C2 domain was found either in small proteins that only contain the C2 fold or associated to different catalytic domains. Some C2 proteins such as synaptotagmins or uncharacterized proteins that combine C2 with the phospholipid-binding GRAM domain also contain a hydrophobic transmembrane domain (dark blue rectangle). Compared to the canonical C2 domain from PKC (130 amino acid residues), the CAR family presents an insertion at the C-terminus (indicated by a black box).

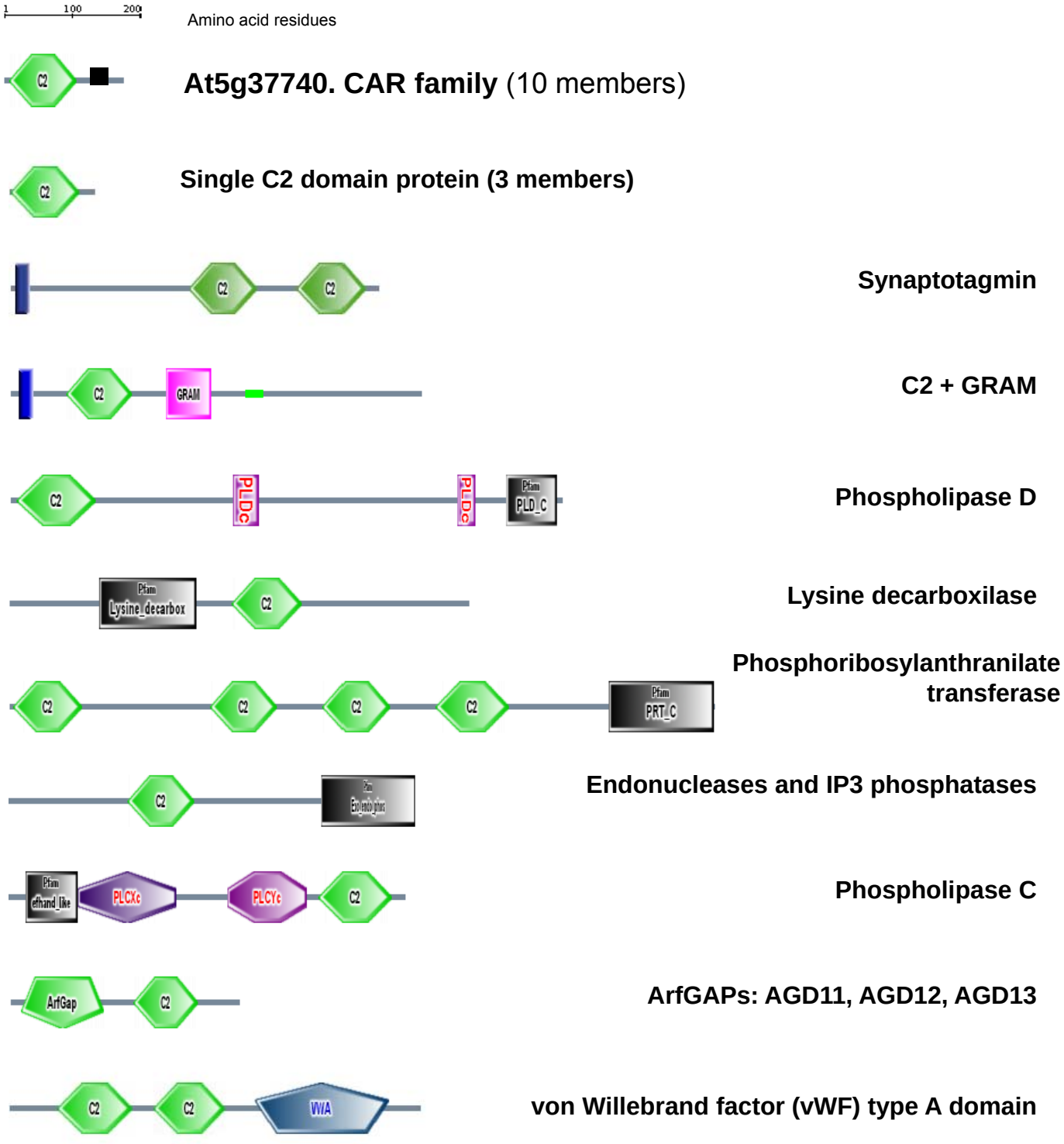

Supplemental Data. Rodriguez et al. Plant Cell (2014) 10.1105/tpc.114.129973

Supplemental Figure 2. Amino acid sequence alignment and cladogram of *Arabidopsis* CAR proteins. **(A)** A family composed by 10 members was revealed by BLAST search at the TAIR database. An alignment was generated using Clustal W program and Genedoc software. The secondary structure of At3g17980 was added to the alignment using ESPript 2.2. The α-helix starting at residue 103 of At3g17980 and the βA and βB sheets represent a singular CAR insertion into the standard C2 fold described previously for PKC or PLC. The loops involved in Ca2+ coordination are indicated as L1, L2 and L3. **(B)** Cladogram of the Arabidopsis CAR family. A tree resulting from the previous alignment was generated using PhyloDraw software.

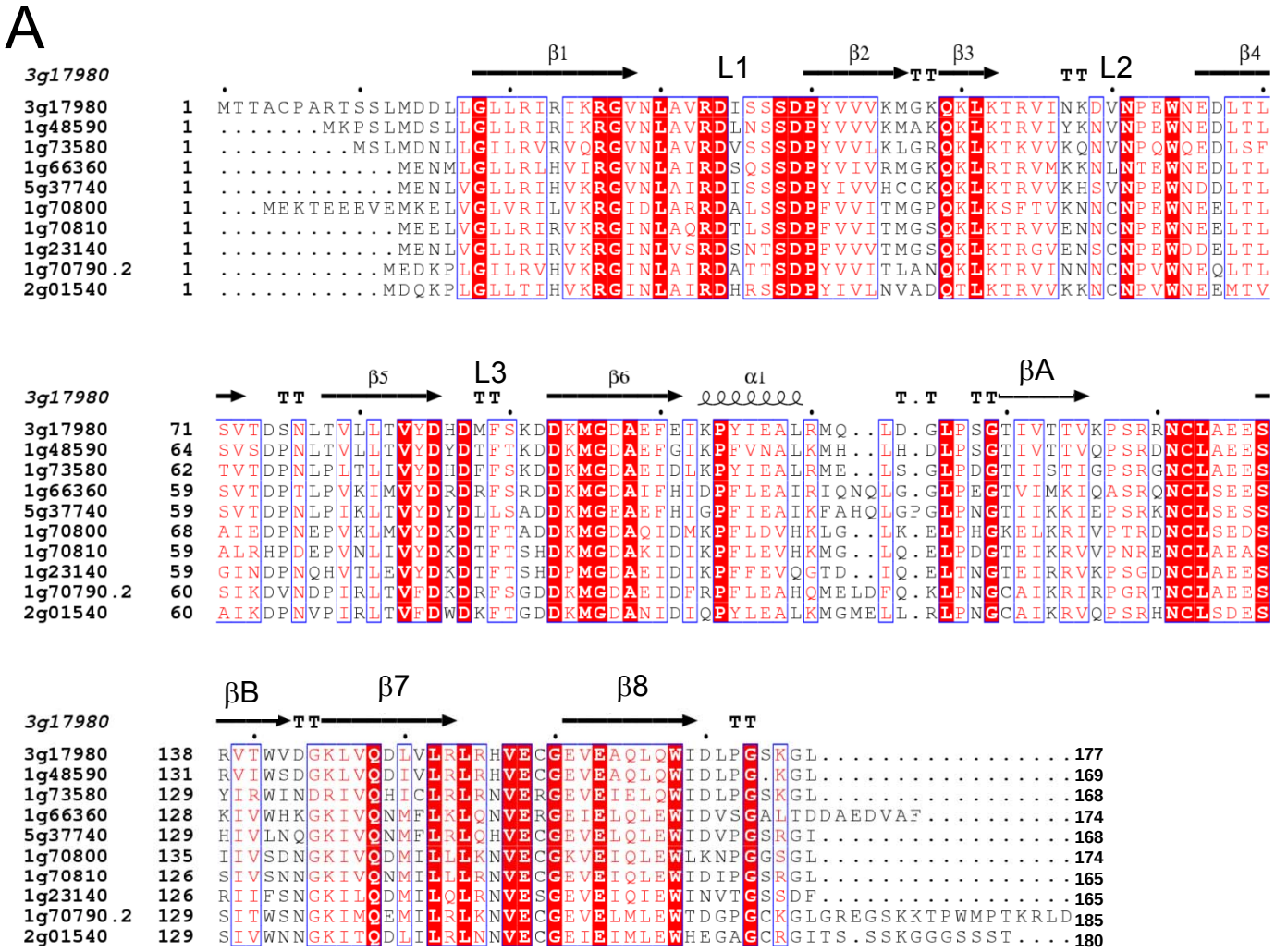

Supplemental Figure 3. Amino acid sequence alignment of representative members of the CAR family in *Arabidopsis*, tomato (*Solanum lycopersicum*) and rice (*Oryza sativa*)

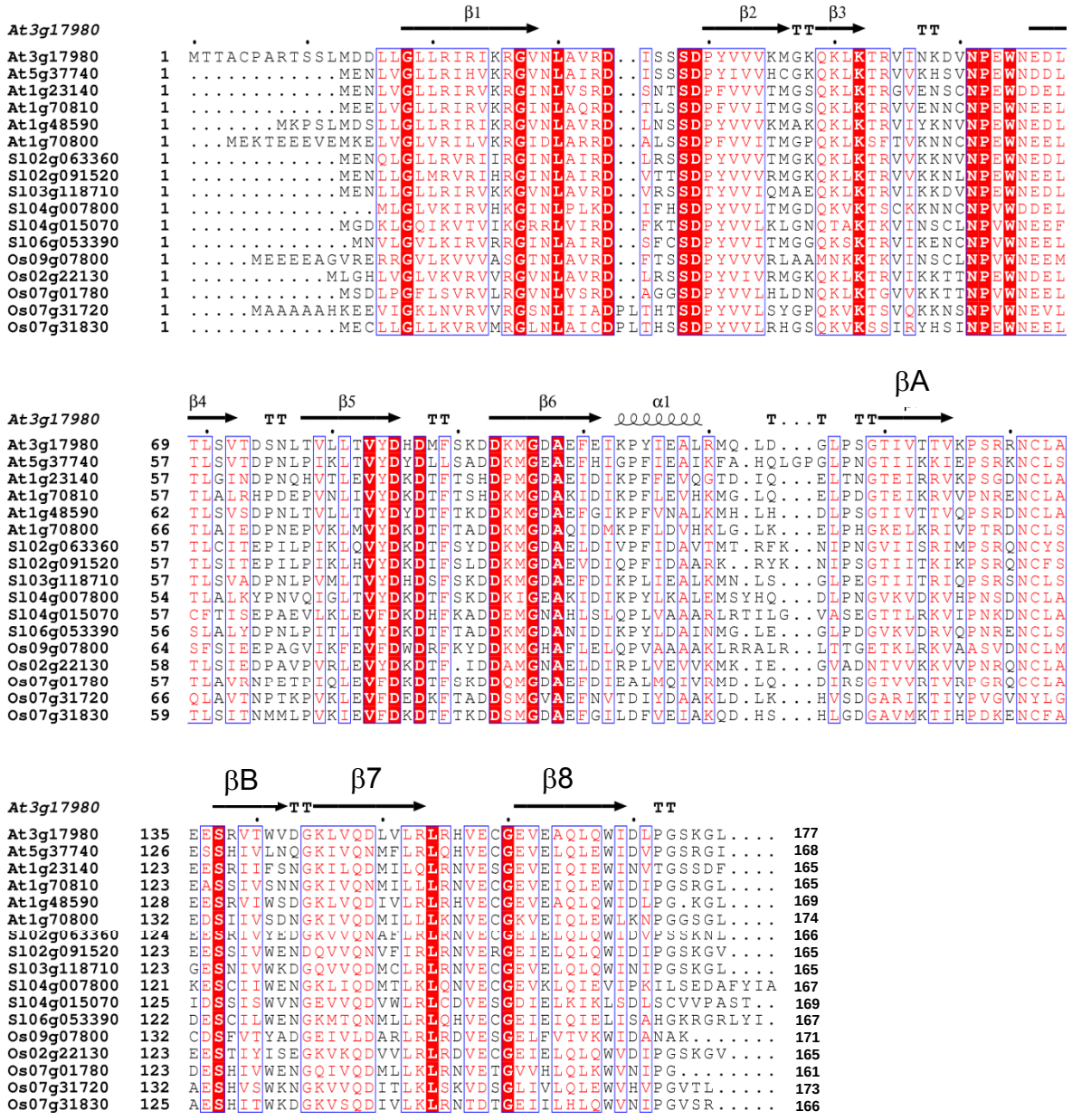

Supplemental Data. Rodriguez et al. Plant Cell (2014) 10.1105/tpc.114.129973

Supplemental Figure 4. Scheme of *CAR1, CAR4, CAR5 and CAR9* genes and location of the corresponding T-DNA insertion in *car* mutants. The position of the primers used for genotyping and RT-PCR analyses are indicated by arrows. Left, RT-PCR analyses of mRNAs extracted from either Col wt seedlings (10 d-old) or the corresponding *car* mutant are shown for each gene; the upper box corresponds to the analysis of each *CAR* gene and the lower box to the *ACTIN* control of cDNA. UTR, untranslated region.

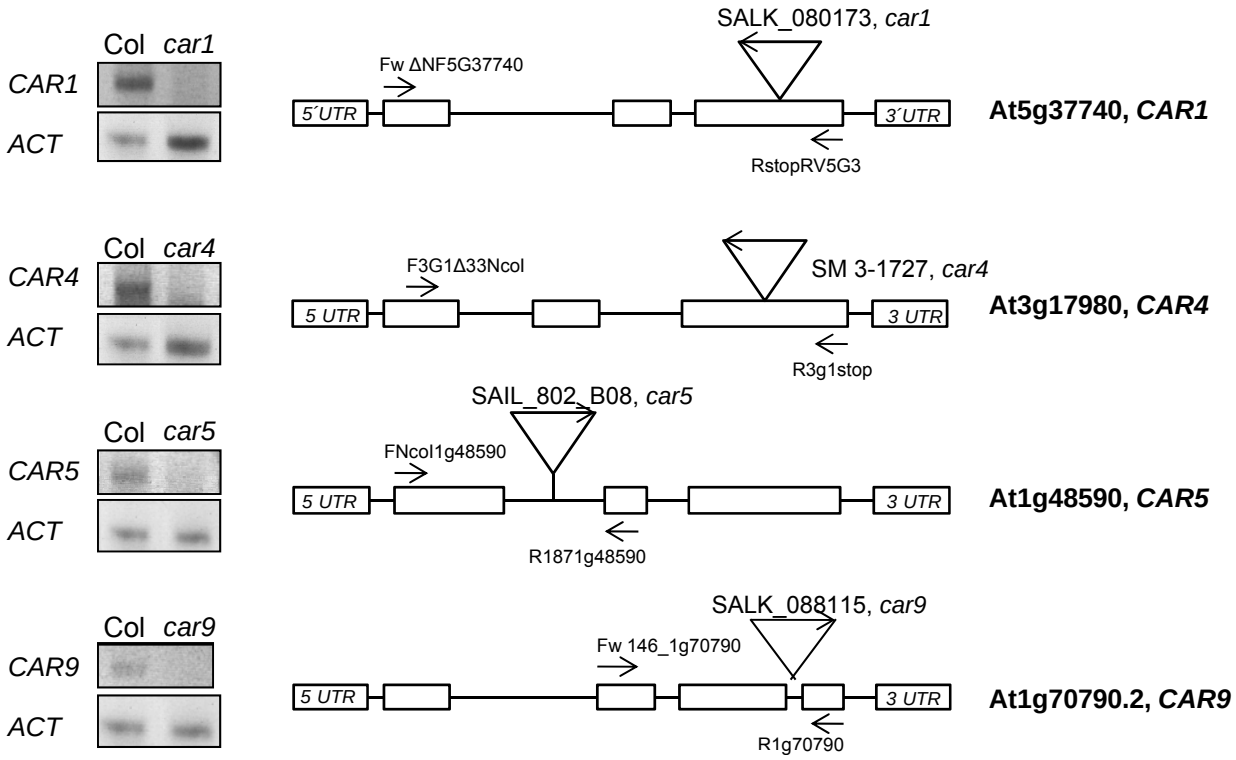

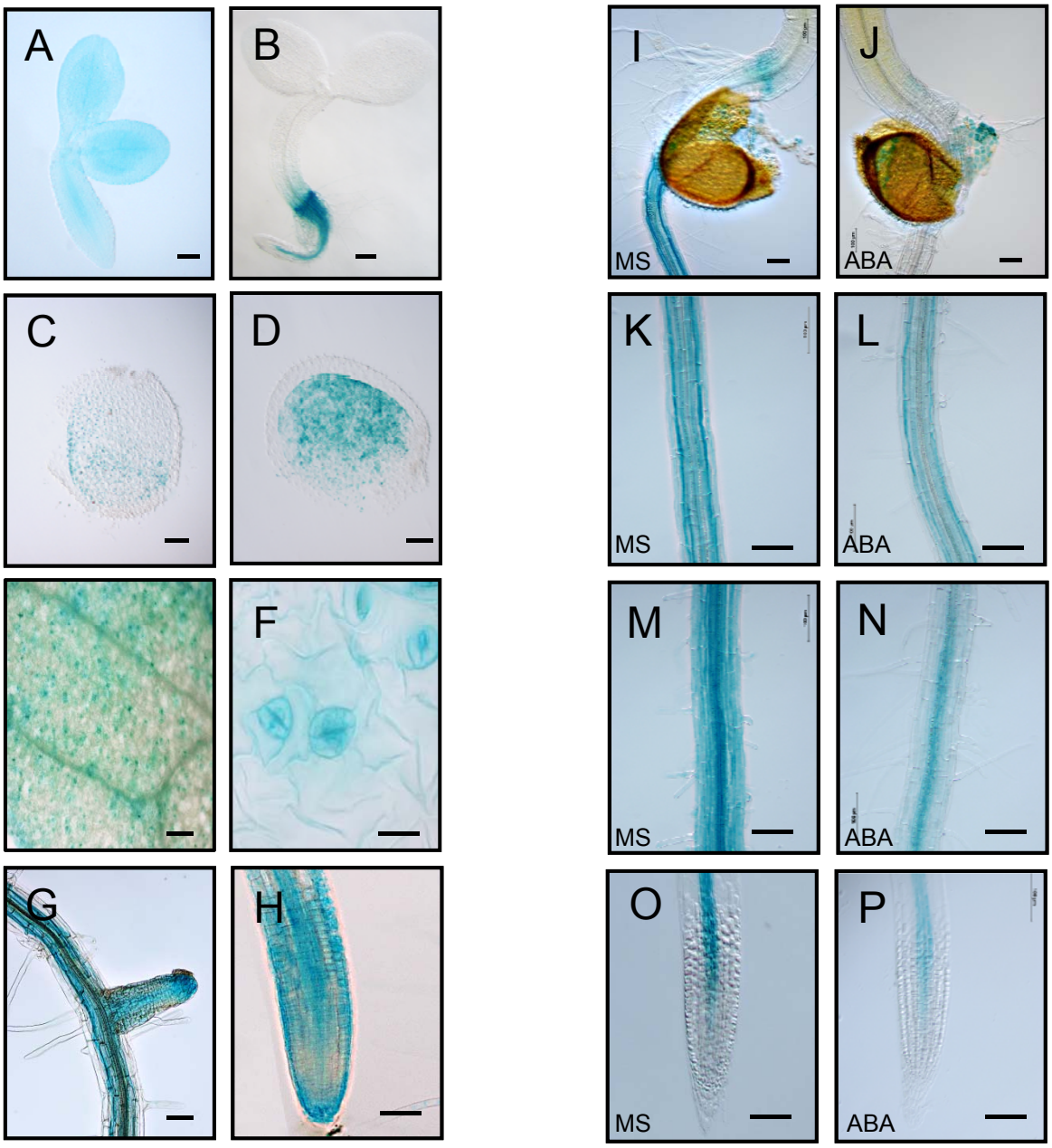

Supplemental Figure 5. Photographs showing GUS expression driven by ProCAR1:GUS gene in different tissues and developmental stages. Bar = 100µm. Generation of ProCAR1:GUS lines and imaging of histochemical GUS staining was performed as described in Gonzalez-Guzman et al., (2012). A fragment comprising 2 kb 5 upstream of the ATG start codon of the CAR1 gene was amplified by PCR and cloned into pMDC163 destination vector.

(A, B) Embryos dissected from mature seeds imbibed for 24 or 48 h, respectively.

(C, D) Dissected seed coat and endosperm imbibed for 4 or 48 h, respectively.

(E, F) Vascular tissue and guard cells in leaves of 8-d-old seedlings, respectively.

(G, H) Emerged lateral roots from 8-d-old seedling.

(I-P) Primary root from 5-d-old seedlings that were mock or 10 µM ABA-treated for 10 h. ABA treatment attenuates GUS expression.

(I, J) Staining of the root-hypocotyl junction.

(K, L) Staining of mature root zone shows CAR1 expression in cortex.

(M-P) Staining of the elongation root zone and root meristem shows predominant expression of CAR1 in vascular tissue.

Supplemental Figure 6. Induction of CAR genes by cold, osmotic and salt stress in shoot or root tissues. Data were obtained from the AtGenExpress data set for abiotic stress-induced gene expression (Kilian et al., 2007). Those *CAR* genes represented in the AtGenExpress data set are shown. Stress treatments were initiated at 18 d after sowing and root and shoot samples were taken at 0, 0.5, 1 , 3, 6, 12 and 24 h after the onset of the treatment. Cold stress was applied by transferring the boxes containing the plants to 4ºC, whereas osmotic and salt stress were applied by transferring rafts containing the plants to MS medium supplemented with 300 mM mannitol or 150 mM NaCl, respectively. Mock-treated plants were used to normalize gene expression data. Red asterisks mark those *CAR* genes that showed at least 2-fold upregulation by stress treatment in any sample.

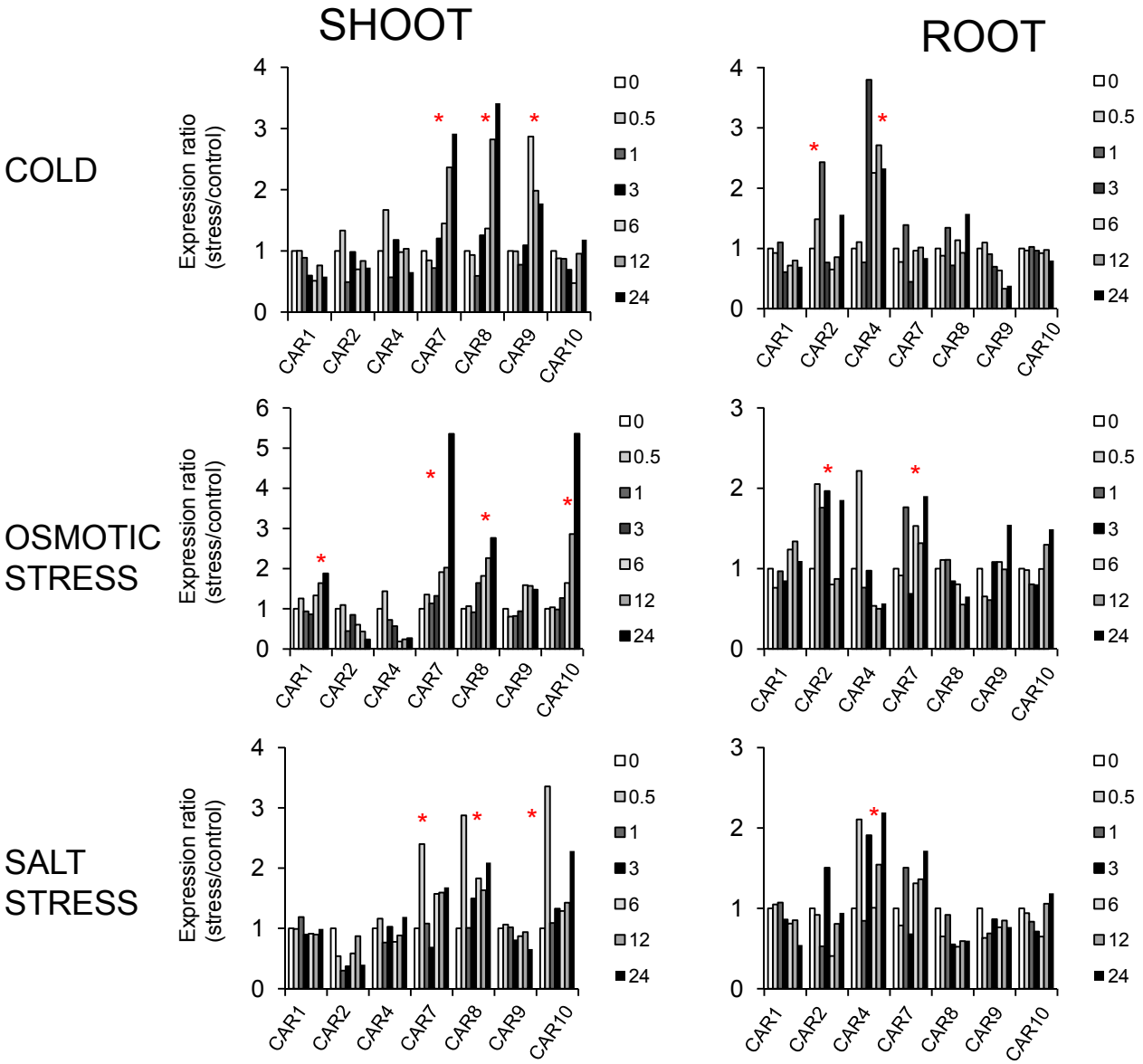

Supplemental Table 1. Data Collection and Refinement Statistics

Data collection	CAR4
Space group	$P2_12_12_1$
Cell dimensions	
a, *b*, *c* (Å)	34.85, 88.14,108,76
Resolution (Å)	46.3-1.60 (1.61-1.60)
R_{sym}, R_{pim}	0.04 (0.24), 0.01 (0.09)
I / σ(I)	37.9 (8.5)
Completeness (%)	99.6 (97.5)
Redundancy	10.3 (8.5)
Refinement	
Number of reflections	84856
R_{work} / R_{free}	19.0 / 22.0 (25.0 / 30.0)
No. atoms	
Protein	2620
Calcium atoms	4
Water molecules	386
R.m.s deviations	
Bond lengths (Å)	0.006
Bond angles (°)	1.092
Ramachandran Plot statistics	98.2 % in the core
	1.8 % in the allowed
	0.0 % outliers

*Highest resolution shell is shown in parenthesis.

$R_{sym} = \Sigma_{hkl} | I_{hkl} - \langle I_{hkl} \rangle | / \Sigma_{hkl} I_{hkl}$

Supplemental Table 2. List of oligonucleotides used in this work

PCR	Primer name	Sequence 5'→ 3'
car1	FΔN5g37740	ATCGTCGTTCACTGCGGTAAAC
	RStpRVBHI5g37740	GGATCCGATATCCTAAATACCCCTTGAACCCGG
T-DNA	LBpROK2	GCCGATTTCGGAACCACCATC
car4	FΔN3g17980	ACCATGGAGGACATCAGTAGCAGCGATCCT
	Rstop3g17980	TCATAGACCCTTGGAGCCAGGGA
T-DNA	Spm3	ACCGTCGACTACCTTTTTTCTTGTAGTG
car5	FNco1g48590	ACCATGGAACCTTCTTTAATGGATAG
	R187_1g48590	CAAGTCTTCATTCCACTCAGGA
T-DNA	LB3SAIL	TAGCATCTGAATTTCATAACCAATCTCGATACAC
car9	F146_1g70790	GTAATCCAGTGTGGAACGAACA
	R1g70790	TTAGTCCAATCGTTTTGTCG
T-DNA	LBpROK2	GCCGATTTCGGAACCACCATC
Transgenic lines	Primer name	Sequence 5'→ 3'
CAR1	FwBHI5g37740	GGATCCATGGAGAATCTTGTAGGTCT
	RStpRVHI5g37740	GGATCCGATATCCTAAATACCCCTTGAACC
pCAR1::GUS	FProm5g37740new	TCAACCACTAGTAGACCACAAATG
	RProm5g37740	–AATTCGAAGAAGACCTACAAGATT
BiFC	Primer name	Sequence 5'→ 3'
CAR1	FwBHI5g37740	GGATCCATGGAGAATCTTGTAGGTCT
	RNStpRVHI5g37740	GGATCCGATATC**CGA**AATACCCCTTGAACC
CAR4	FATGNco3g17980	ACC ATG GCA ACG GCG TGT CCG GCG
	RnostopRV3g17980	GATATCTGATAGACC CTTGGAGCCAGGG
CAR5	FNco1g48590	ACCATGGAACCTTCTTTAATGGATAG
	RnostopRV1g48590	GATATCTGATAGACCCTTTCCGGGAAGATC
Mutants	Primer name	Sequence 5'→ 3'
$CAR1^{D22A\ D27A}$	FwD22A D27A	GCCATTAGA**gcc**ATCTCAAGCAGT**gct**CCTTACATC
	RvD22A D27A	GATGTAAGG**agc**ACTGCTTGAGAT**ggc**TCTAATGGC
$CAR4^{D85A\ D87A}$	FwD85A D87A	ACGGTGTAT**gct**CAC**gcc**ATGTTTAGC
	RvD85A D87A	GCTAAACAT**ggc**GTG**agc**ATACACCGT
$CAR4^{\Delta ED}$	FwEAL	GAGATAAAGCCCAGTGGTGTCGACGGCAAGCTCGTCCAGGAT
	RvVTW	GACGAGCTTGCCGTCGACACCACTGGGCTTTATCTCGAACTCAG CATCGCC
Y2H	Primer name	Sequence 5'→ 3'
PYR1	FNc4g17870	ACCATGGCTTCGGAGTTAACACCA
	R4g17870	TCACGTCAC CTGAGAACCACT
PYL1	FNco5g46790	ACCATGGCGAATTCAGAGTCCTC
	RBamHI46790	GGATCCTTACCTAACCTGAGAAGAGTTGT
Δ1-47 PYL4	FGPN2g38310	ACCATGGGTCCTAATCAGTGTTGCTCC
	R2g38310	CGCACGAATTCACAGAGACATCTTCTTCTT
PYL6	FNcoI2g403	ACCATGGCGAATTCAGAGTCCTC
	R2g040330	GGATCCTTACCTAACCTGAGAAGAGTTGT
Δ1-47 PYL6	FNc2g403	ACCATGGAGCACGTGGAGCTTTCCCAC
	R2g040330	GGATCCTTACCTAACCTGAGAAGAGTTGT
Δ1-27 PYL8	FwDNNcoPYL8	ACCATGGTGGATAATCAGTGTAGCTCT
	RvESRVpyl8	TTAGACTCTCGATTCTGTCGT

Supplemental Methods

Data Collection and Structure determination and refinement

CAR4 X-ray diffraction data was collected in a ADSC detector using the European Synchrotron Radiation Facility (Grenoble, France) radiation source at 0.94 Å wavelengths at the ID14.4 beamline. Diffraction data was processed with XDS (Kabsch, 2010) and scaled with SCALA from the CCP4 package (Collaborative Computational Project, Number 4) (Winn et al., 2011). A summary of the data-collection statistics is given in Supplemental Table 1 online. The X-ray structure of CAR4 was solved by molecular replacement using the coordinates of the X-ray structure of the C2 domain of Munc13-C2b (Protein Data Bank code 3KWT) as the search model (Shin et al., 2010; Vagin and Isupov, 2001). The electron density map calculated using these phases was good enough to manually build and refine the residues of CAR4. Several cycles of restrained refinement with REFMAC5 (Murshudov et al., 2011) and PHENIX (Adams et al., 2010) and iterative model building with COOT (Emsley et al., 2010) were carried out. The stereochemistry of the model was verified with PROCHECK (Laskowski et al., 1996). Ribbon figures were produced using PyMOL (http://www.pymol.org). The refinement statistics are summarized in Supplemental Table 1 online.

GUS staining

Histochemical GUS staining was performed as described previously (Antoni et al., 2013).

Supplemental References

Adams, P. D., Afonine, P. V., Bunkoczi, G., Chen, V. B., Davis, I. W., Echols, N., Headd, J. J., Hung, L. W., Kapral, G. J., Grosse-Kunstleve, R. W., McCoy, A. J., Moriarty, N. W., Oeffner, R., Read, R. J., Richardson, D. C., Richardson, J. S., Terwilliger, T. C., and Zwart, P. H. (2010). PHENIX: a comprehensive Python-based system for macromolecular structure solution. Acta Crystallogr.D.Biol.Crystallogr. **66**, 213-221.

Antoni, R., Gonzalez-Guzman, M., Rodriguez, L., Peirats-Llobet, M., Pizzio, G. A., Fernandez, M. A., De Winne, N., De Jaeger, G., Dietrich, D., Bennett, M. J., and Rodriguez, P. L. (2013). PYRABACTIN RESISTANCE1-LIKE8 plays an important role for the regulation of abscisic acid signaling in root. Plant Physiol **161**, 931-941.

Emsley, P., Lohkamp, B., Scott, W. G., and Cowtan, K. (2010). Features and development of Coot. Acta Crystallogr.D.Biol.Crystallogr. **66**, 486-501.

Kabsch, W. (2010). XDS. Acta Crystallogr.D.Biol.Crystallogr. **66**, 125-132.

Laskowski, R. A., Rullmannn, J. A., MacArthur, M. W., Kaptein, R., and Thornton, J. M. (1996). AQUA and PROCHECK-NMR: programs for checking the quality of protein structures solved by NMR. J.Biomol.NMR **8**, 477-486.

Murshudov, G. N., Skubak, P., Lebedev, A. A., Pannu, N. S., Steiner, R. A., Nicholls, R. A., Winn, M. D., Long, F., and Vagin, A. A. (2011). REFMAC5 for the refinement of macromolecular crystal structures. Acta Crystallogr.D.Biol.Crystallogr. **67**, 355-367.

Shin, O. H., Lu, J., Rhee, J. S., Tomchick, D. R., Pang, Z. P., Wojcik, S. M., Camacho-Perez, M., Brose, N., Machius, M., Rizo, J., Rosenmund, C., and Sudhof, T. C. (2010). Munc13 C2B domain is an activity-dependent Ca2+ regulator of synaptic exocytosis. Nat.Struct.Mol.Biol. **17**, 280-288.

Vagin, A. A. and Isupov, M. N. (2001). Spherically averaged phased translation function and its application to the search for molecules and fragments in electron-density maps. Acta Crystallogr.D.Biol.Crystallogr. **57**, 1451-1456.

Winn, M. D., Ballard, C. C., Cowtan, K. D., Dodson, E. J., Emsley, P., Evans, P. R., Keegan, R. M., Krissinel, E. B., Leslie, A. G., McCoy, A., McNicholas, S. J., Murshudov, G. N., Pannu, N. S., Potterton, E. A., Powell, H. R., Read, R. J., Vagin, A., and Wilson, K. S. (2011). Overview of the CCP4 suite and current developments. Acta Crystallogr.D.Biol.Crystallogr. **67**, 235-242.